

Fast and Slow Stages of Lifetime Degradation by Boron–Oxygen Centers in Crystalline Silicon

Jan Schmidt,* Karsten Bothe, Vladimir V. Voronkov, and Robert Falster

A conflict between previous and recently published data on the two-stage light-induced degradation (LID) of carrier lifetime in boron-doped oxygen-containing crystalline silicon is addressed. The previous experiments showed the activation of two boron–oxygen recombination centers with strongly differing recombination properties for the fast and slow stages of LID, whereas more recent studies found only a single center for both stages. To resolve this controversy, the historic silicon samples of these previous examinations are re-examined in this study after more than one decade. It is found that, in the historic samples, the fast stage can be either described by two different centers or a mixture of the two, depending on the duration of previous dark annealing. A possible solution is suggested based on the involvement of different activating impurities in the boron–oxygen defect. In dark-annealed samples, the defect consisting of boron, oxygen, and the activation impurity is present in two latent configurations, which reconfigure during LID at a fast and a slow stage. In the examined historic silicon samples, which did not undergo a gettering pretreatment, a significant concentration of an additional boron–oxygen defect with a different kind of activating impurity attached exists. The historic and modern results are thus reconciled.

1. Introduction

The carrier lifetime in boron-doped and oxygen-containing silicon is long known^[1–5] to degrade severely in the presence of excess electrons. This phenomenon, crucial for solar cell efficiency,^[5–7] is often referred to as light-induced degradation (LID), although the actual reason for the effect is not the light itself but the excess carriers. LID was found also in n-type silicon containing boron,^[8–13] but in the present paper, the discussion is limited to boron-doped p-type silicon. Note that most recently, different degradation effects under illumination have been reported, in particular, in multicrystalline silicon solar cells,^[14–17] which are not part of this study. In the following the abbreviation “LID” is hence restricted to the boron–oxygen (B–O)-related kind of degradation.

LID proceeds in two stages—a fast one and a slow one.^[4,18] The rate constant was initially found^[4] to be proportional to the squared boron concentration and later was shown^[12,19–21] to be actually proportional to the squared hole concentration p^2 . The rate constant was found to be independent of electron concentration n , with an exception of a very low n corresponding to light intensities less than 0.01 sun.^[5] This has been explained^[12] by a two-step process, occurring at each degradation stage: the first step is controlled by holes and the second one by electrons. The second step is rate-limiting only at a very low n . The hole concentration p is close to the boron concentration $[B]$ for boron-only doped material and at low injection levels. The degradation rate constants also slightly depend on the temperature. At T_{room} (about 25 °C) and at $[B] = 10^{16} \text{ cm}^{-3}$ (which is a typical doping level for a silicon solar cell wafer), the timescales are $t_f = 15 \text{ s}$ and $t_s = 3.5 \text{ h}$, for the fast and slow stages, respectively.^[4] For lower doping levels, both timescales become essentially longer.

Based on these features, it was suggested^[22] that the B–O defects responsible for LID are initially present in a recombination-inactive state denoted as latent center (LC) and that the degradation occurs by an electron-assisted reconfiguration of LC into a recombination-active state, RC, of the same B–O defect.


A complicating feature is that the RCs found at the fast stage and those found at the slow stage possess different recombination properties,^[4] implying that there are two different kinds of RCs, denoted as the fast-stage recombination center (FRC) and slow-stage recombination center (SRC) in the past. The two types

Prof. J. Schmidt, Dr. K. Bothe
Department of Photovoltaics
Institute for Solar Energy Research Hamelin (ISFH)
Am Ohrberg 1, Emmerthal 31860, Germany
E-mail: j.schmidt@isfh.de

Prof. J. Schmidt
Department of Solar Energy
Institute of Solid-State Physics
Leibniz University Hannover
Appeltr. 2, Hannover 30167, Germany

Dr. V. V. Voronkov
Global Wafers
via Nazionale 59, Merano 39012, Italy

Dr. R. Falster
4 Harrison's Lane, Woodstock OX20 1SS, UK

 The ORCID identification number(s) for the author(s) of this article can be found under <https://doi.org/10.1002/pssb.201900167>.

© 2019 The Authors. Published by WILEY-VCH Verlag GmbH & Co. KGaA, Weinheim. This is an open access article under the terms of the Creative Commons Attribution-NonCommercial-NoDerivs License, which permits use and distribution in any medium, provided the original work is properly cited, the use is non-commercial and no modifications or adaptations are made.

DOI: 10.1002/pssb.201900167

of RCs are characterized by strongly different injection-level dependencies.^[4,12] The fast and slow degradation may occur sequentially or in parallel.

In forward-biased solar cells,^[23] the fast degradation process is negligible at a small applied voltage of 0.4 V (at a low n), but the slow one occurs at a normal rate. This is in accordance with a *parallel production* of FRC and SRC, that is, each RC originates from its own latent precursor: the fast latent center (FLC) is a precursor for FRC, and slow latent center (SLC) is a precursor for SRC, as shown schematically in **Figure 1a**. All the centers in Figure 1 are just different configurations of the same B–O defect family.

If the degraded silicon samples are annealed in the dark, in a range between 100 and 200 °C, the lifetime recovers^[2,18,24] back to the predegradation value τ_0 . This is explained by a backward reconfiguration of FRC and SRC into their latent forms that are dominant under equilibrium conditions. However, this reconfiguration is not as simple as just the backward transitions from FRC to FLC and SRC to SLC, respectively. It was found^[4] that the fast-stage degradation of the open-circuit voltage of a solar cell is quickly recovered already near room temperature T_{room} —within a time-scale of 15 min—but the recovery is only partial, by about 50%. Full recovery occurs only at higher T at a rate representative of annealing of the SRC. An obvious interpretation of this is that, in the dark, the FRC is quickly converted into SRC; a partial lifetime recovery means that the FRC is a somewhat more efficient recombination center (RC) than the SRC, at the same concentration. The complete recovery scheme is shown in **Figure 1b**. In fully recovered samples, the two latent defects coexist in an equilibrium ratio, and a subsequent (repeated) degradation occurs in the same way as for the first degradation run.

Recently reported data^[25–28] confirmed a two-stage degradation, with similar timescales as reported in the study by Bothe and Schmidt,^[4] for the fast and slow stage, respectively. However, these data are in a severe contradiction with the degradation/recovery scenario of **Figure 1**. First, the same kind of RC (similar to SRC) was found in both fast and slow degradation stages, judging by the injection-level dependence of the lifetime.

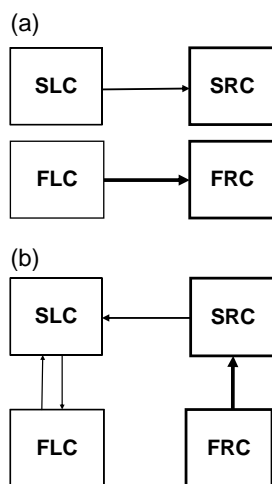


Figure 1. Schematic transitions between the LCs (FLC and SLC) and the RCs (FRC and SRC) for a) degradation and b) dark recovery.

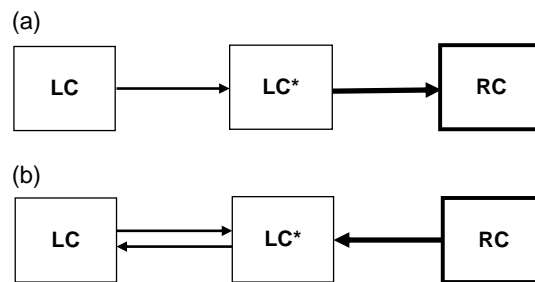


Figure 2. Sequential scenario^[25–27] for a) degradation and b) dark recovery that involves two LCs (LC and LC*) and a single RC.

The second impressive finding was that if a dark anneal at 200 °C is significantly shorter than the 10 min typically used for this process (like 10 s—just sufficient to recover the lifetime), the subsequent degradation occurs almost entirely within a fast stage. This behavior has been explained^[25–27] by a sequential scenario shown in **Figure 2a**—with two recombination-inactive latent defects denoted here as LC and LC*; the latter one is an immediate precursor for production of RC. In samples annealed in the dark for a sufficiently long time, the two latent states are equilibrated, and the LC state is dominant. The fast stage is a conversion of the minor state LC* into RC. Major degradation occurs within a slow stage, by the conversion of LC into LC* (with subsequent quick conversion into RC). A short dark anneal leads to a backward conversion of RC into the immediate precursor LC* (Figure 2b), which creates a strongly non-equilibrium population of the latent defects: mostly LC*. The subsequent degradation is then a one-stage fast conversion, $\text{LC}^* \rightarrow \text{RC}$.

A completely identical behavior would occur also within a parallel scheme of degradation/recovery (**Figure 3**). Here the fast degradation stage is again a quick conversion of LC* into the RCs, and the slow stage is a direct production of RC from LC. A short dark anneal of a degraded sample leads to a backward conversion of RC into LC* along a fast path (Figure 3b), and a longer anneal leads to equilibration between LC* and LC. A repeated degradation occurs completely within a fast stage for a short dark anneal and in a two-stage mode for a long anneal.

The puzzling controversy between the historic and the recent data will be now addressed. To clarify the situation, the “old” historic samples—the same that were inspected previously^[4,5] and were then stored in the dark for more than 14 years—were re-examined.

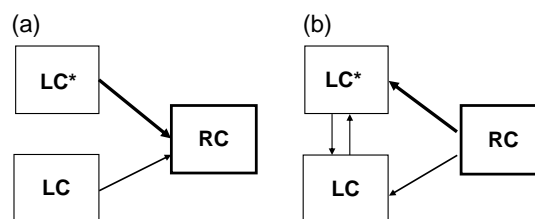


Figure 3. Parallel scenario involving two LCs (LC and LC*) and a single RC: a) degradation and b) dark recovery.

2. Experimental Section

Surface passivation of the “historic” boron-doped Czochralski-silicon (Cz-Si) samples was performed by the plasma-enhanced chemical vapor deposition of silicon nitride layers on both wafer surfaces. The samples were not phosphorus gettered and received only chemical cleaning before surface passivation. It can hence be conjectured that the historic material contains somewhat higher concentrations and a different mix of residual metallic impurities compared with the modern state-of-the-art-gettered Cz-Si material. Further details on the sample processing of the historic samples can be found in the study by Bothe and Schmidt.^[4] The historic samples (of $p_0 = 5.2 \times 10^{15} \text{ cm}^{-3}$) were examined in three different states in the study by Bothe and Schmidt:^[4] a nondegraded state (reached after dark annealing at 200 °C), a state after completion of the fast degradation stage (200 s of halogen lamp illumination), and the state after full degradation (after 60 h of illumination). At the time of the previous studies,^[4] the three states were characterized by strongly differing lifetimes τ , corresponding to the undegraded, the partially degraded, and the fully degraded state. Remeasured directly after 14 years of storage in the dark, the samples interestingly showed the lifetime τ_0 as representative of the nondegraded dark-annealed state. The dark recovery time^[24] extrapolated down to T_{room} amounts to ≈ 30 years, which is, however, a very rough estimate due to spanning through many orders of magnitude. Therefore, the observed lifetime dark recovery during the long 14 years of storage in the dark is consistent with the previously reported data for the recovery rate within the reported uncertainty range.

These historic samples (as well as control modern Cz-Si samples) were first dark annealed at 200 °C for 10 min. To re-examine the dynamics of the degradation process, the lifetime was first measured as a function of the illumination time using the microwave-detected photoconductance decay (MW-PCD) technique (Semilab, WT-2000) at a fixed bias illumination intensity (halogen lamp) of 0.25 suns. In a subsequent experiment, the samples were annealed again at 200 °C in darkness and the injection-level dependence of the lifetime was measured before and during the course of degradation (for a selected set of illumination times corresponding to the three states mentioned earlier) using a Sinton lifetime tester (WCT-120) via the generalized analysis. The fully degraded samples were then dark-annealed again, for various durations (10 s–60 min), and the degradation experiments were repeated. The observed lifetime degradation behavior was always fully reproducible after dark annealing.

2.1. Degradation in Dark-Annealed “Historic” Cz-Si Samples

During LID, the reciprocal measured lifetime $1/\tau$ is incremented with respect to the value $1/\tau_0$ measured before a degradation run due to the increasing concentration of RCs activated. The lifetime component due to RCs can thus be calculated through the measured lifetimes^[2,29] by

$$1/\tau_{\text{RC}} = 1/\tau - 1/\tau_0 \quad (1)$$

Equation (1) of course assumes that other essential recombination channels (not related to B–O defects—like surface

recombination) are not affected by illumination; this was confirmed in the past^[4] by processing Float-zone silicon (Fz-Si) samples (with a negligible amount of B–O) along with the inspected samples. In addition, the full reproducibility of the degradation behavior after 200 °C dark annealing, which we observed in this study, is another clear indication that the other recombination channels do not change during illumination. In particular, a possible effect of the light-induced dissociation of iron–boron pairs was checked (Section 2.4) and found inessential.

The lifetime τ_{RC} , due to a single-level deep center, is a linear function^[12,30] of the ratio n/p of the carrier concentrations:

$$\tau_{\text{RC}} = (1 + Qn/p)/A \quad (2)$$

where Q is the ratio of the capture coefficients of electrons and holes, α_n/α_p . The recombination amplitude A is equal to $\alpha_n M$, where M is the center concentration. If the energy level of RC is not deep, the thermal emission of carriers should be taken into account. The functional dependence of Equation (2) is then retained^[12,30] but the parameters Q and A become dependent on p_0 .

The B–O defect is actually a two-level center existing in three charge states.^[12,13] The lifetime dependence on n/p is thus more complicated and nonlinear.^[12,30] However, in p-type silicon, this dependence is reduced^[12] to that expected for a one-level deep donor center—and represented by a simple Equation (2).

By previous studies,^[4,12] the dependence of τ_{RC} on n/p is indeed linear for both FRC and SRC; the ratio Q is about 10 for the SRC and much larger (about 100) for the FRC. Note that the linear dependence follows from simply replotting the data from the study by Bothe and Schmidt^[4] (τ and τ_0 in dependence of n)—now as a dependence of $1/\tau_{\text{RC}} = 1/\tau - 1/\tau_0$ over n/p .

In remeasuring the historic samples 14 years later, we can now confirm that when these samples were dark annealed for 10 min, degradation indeed occurs in two stages (Figure 4, curve 1), as previously found.^[4] For a short dark anneal, however, for 10 s or 1 min, degradation occurs almost entirely within a fast stage, with a timescale of about 100 s (Figure 4, curve 2)—in accordance with recent findings.^[25–27]

2.2. Injection-Level Dependence of the RC Lifetime for the Historic Samples

The RC lifetime calculated by Equation (1) in samples annealed for a short time (10 s or 1 min) shows a linear dependence on n/p (Figure 5), and the deduced capture ratio Q is close to 11 for all the probed illumination times. This is the same value that was found for the SRC. Therefore, the RC that was previously labelled SRC is not specific only for a slow stage of degradation but can be also the major center during a fast stage. For this reason, the notation should be modified: hence, from now on we label this RC as RC₁.

The amplitude A_1 of the RC₁ center was deduced from the curves of Figure 5 using Equation (2), and the time dependence of A_1 is shown in Figure 6. In spite of the small number of data points, a two-stage increase in A_1 is evident, with a small but appreciable slow component. This means that an anneal for 1 min is already sufficient to partially populate the LC state, by transition from LC* to LC in Figure 2 or 3. The time dependence is well fitted by a double-exponential equation:

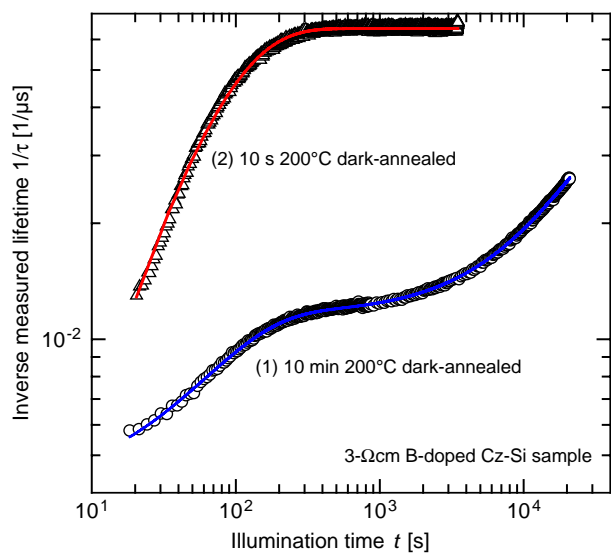


Figure 4. Inverse lifetime $1/\tau$ measured by MW-PCD as a function of time t during illumination with a halogen lamp (0.25 suns) at T_{room} ; curves 1 and 2 are for dark 200 °C preanneal for 10 min and 10 s, respectively. The Cz-Si sample is the same as shown in Figure 2 in the study by Bothe and Schmidt.^[4] The solid lines shown are exponential rise-to-maximum fits (double exponential in the case of curve 1, monoexponential for curve 2) to the measured data.

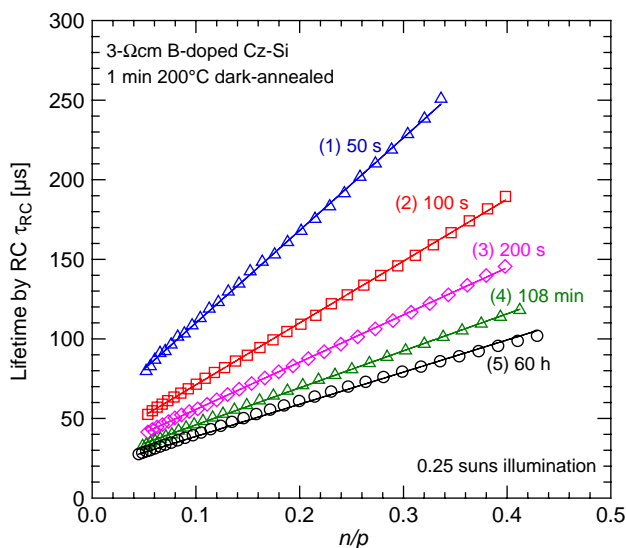


Figure 5. Injection-level dependence of the lifetime by the illumination-induced RC τ_{RC} calculated using Equation (1) for the historic 3 Ωcm boron-doped Cz-Si sample of Figure 4, preannealed in the dark at 200 °C for 1 min and then illuminated at T_{room} at a light intensity of 0.25 sun. The curves 1–5 are for different illumination times: (1) 50 s, (2) 100 s, (3) 200 s, (4) 108 min, and (5) 60 h, respectively.

$$A_1(t) = A_{1f}[1 - \exp(-t/t_f)] + A_{1s}[1 - \exp(-t/t_s)] \quad (3)$$

The deduced time constants are $t_f = 1.25$ min and $t_s = 200$ min, for the fast and slow stages, respectively. The relative contribution of the fast process (of the LC* state) to lifetime degradation

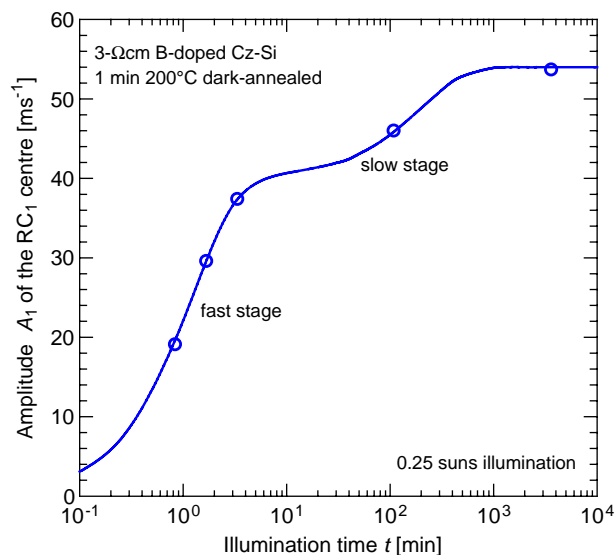


Figure 6. Evolution of the amplitude A_1 of RC₁ as deduced from the curves shown in Figure 5 using Equation (2). The solid blue line is the double-exponential fit of Equation (3) to the measurement data shown as open circles. The time constants extracted from the fit are $t_f = 1.25$ min for the fast and $t_s = 200$ min for the slow stages.

is equal to $A_{1f}/(A_{1f} + A_{1s})$. After a 1 min dark anneal, it is dominant—about 75%, implying that the conversion time from LC* to LC is well longer than 1 min at 200 °C.

For samples preannealed for a longer time (3 or 5 min), the dependence of τ_{RC} on n/p is also linear for all the illumination times (Figure 7), but the apparent parameter Q is now time dependent: it is 80 for the shortest illumination (100 s) and

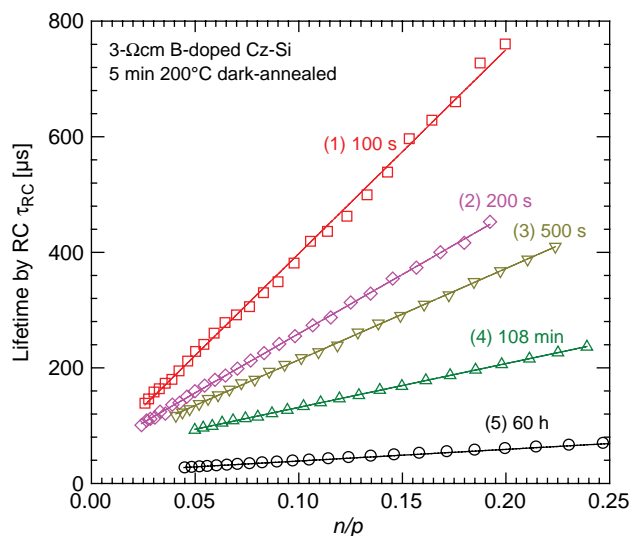


Figure 7. Injection-level dependence of the lifetime by the illumination-induced RC τ_{RC} calculated by Equation (1) for the historic 3 Ωcm boron-doped Cz-Si sample of Figure 4, preannealed in the dark at 200 °C for 5 min and then illuminated at T_{room} at a light intensity of 0.25 suns. The curves 1–5 are for different illumination times: (1) 100 s, (2) 200 s, (3) 500 s, (4) 108 min, and (5) 60 h, respectively.

gradually decreases down to 11 upon increasing the illumination time. The solid curves in Figure 7 are the fitted ones according to a model described in the following sections.

For samples preannealed for 10 min, the $\tau_{RC}(n/p)$ function is super-linear after incomplete degradation, following illumination for 200 s (Figure 8, curve 1), and linear after complete degradation for 60 h (curve 2 corresponding to $Q = 11$).

For a still longer preanneal time (60 min), an illumination for 50 s leads not to a degradation (a reduction in τ) but to some increase in τ (Figure 9), showing that some RCs seem to disappear under illumination. Only for a longer illumination does the lifetime decrease.

2.3. Injection-Level Dependence of the RC Lifetime for Modern Cz-Si Samples

The measurement procedure described earlier was applied to modern phosphorus-gettered B-doped Cz-Si samples (of $p_0 = 1.1 \times 10^{16} \text{ cm}^{-3}$). Again, degradation proceeds in two stages for a long dark preanneal (10 min) but within one (fast) stage for a short dark preanneal (10 s). For all illumination times, only one kind of RC (RC_1 of $Q = 11$) was found. This result is similar to that recently published,^[25–28] although the reported value of the capture ratio Q was larger, 19, in accordance with other data.^[31,32] Note that in these papers, however, the injection-dependent lifetimes were fitted using a two-level defect model, whereas we use a one-level approach here. The use of one-level fitting is very convenient and allows for good comparison with literature data. The validity of a single-level approximation to the multilevel B–O defect in p-type silicon has been discussed in detail previously.^[12] We have hence recalculated the value of Q using the raw data for τ_0 and τ as in Figure 7 in the study by Kim et al.^[27] and determined $Q = 15$ using the single-level approach, which is still

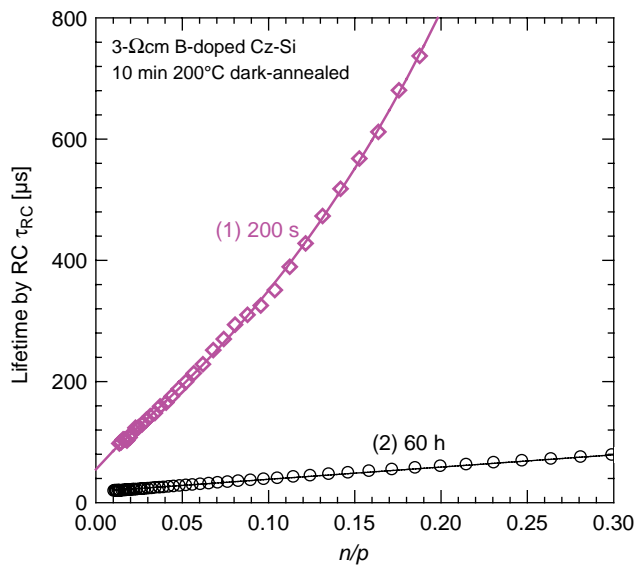


Figure 8. Injection-level dependence of the lifetime τ_{RC} calculated by Equation (1) for the historic 3 Ω cm boron-doped Cz-Si sample of Figure 4, preannealed at 200 °C for 10 min and then illuminated at T_{room} , at a light intensity of 0.25 suns. The curves 1 and 2 are for illumination times of 200 s and 60 h, respectively.

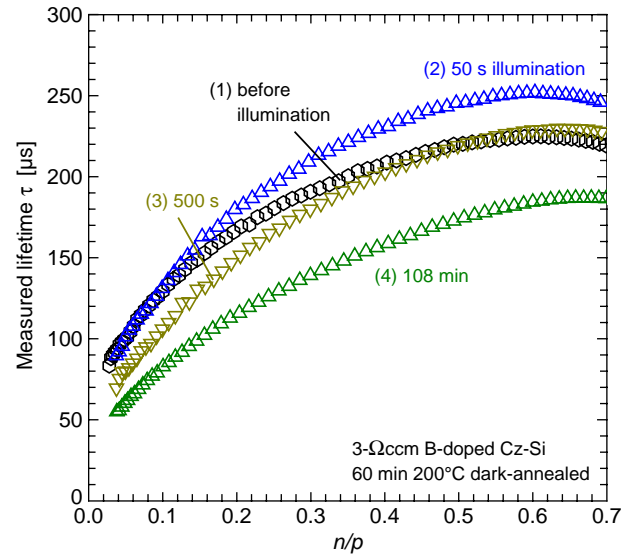


Figure 9. Measured effective lifetime τ as a function of n/p for the historic 3 Ω cm boron-doped Cz-Si sample of Figure 4, preannealed in the dark at 200 °C for 60 min and then illuminated at T_{room} at a light intensity of 0.25 suns. The curves 1–4 are for different illumination times: (1) before illumination (0 s), (2) 50 s, (3) 500 s, and (4) 108 min, respectively.

larger than the Q value extracted from our measurements, 11. In a more recent publication,^[33] a corrected value of Q close to 12 was reported for the single-level approach, which is now similar to our value of 11. Note that we estimate the uncertainty in our experimentally determined Q values to be around $\pm 10\%$.

2.4. Test for a Possible Iron Effect on Measured Lifetime

A large apparent value of the capture ratio Q for the FRC in the study by Bothe and Schmidt^[4] was conjectured^[25–28] to be related not to the production of a specific center (FRC) but rather to the production of the SRC (RC_1) accompanied by a light-induced dissociation of FeB pairs. In view of this possibility, we have checked the iron effect on lifetime, applying the following procedure to the historic samples of Figure 4. The sample was annealed at 200 °C for 10 min in the dark, which results in the dissociation of most of the FeB pairs.^[34] The equilibrium fraction of the remaining FeB is 30% at this T and for a boron concentration of $5 \times 10^{15} \text{ cm}^{-3}$. Then, the sample was quenched and aged in the dark at T_{room} for 20 h, which is more than enough^[34] for complete trapping of iron by boron. The lifetime was measured before and after aging. A conversion of some Fe (with a contribution $1/\tau_{Fe}$ into the reciprocal lifetime $1/\tau$) into an equal amount of FeB (with a contribution $1/\tau_{FeB}$ into $1/\tau$) leads to an increment in the reciprocal lifetime of

$$\Delta(1/\tau) = 1/\tau_{FeB} - 1/\tau_{Fe}. \quad (4)$$

This expected increment, calculated with the recombination parameters of FeB and Fe taken from the study by Macdonald et al.^[35], is shown in Figure 10 as a solid line, depending on n/p .

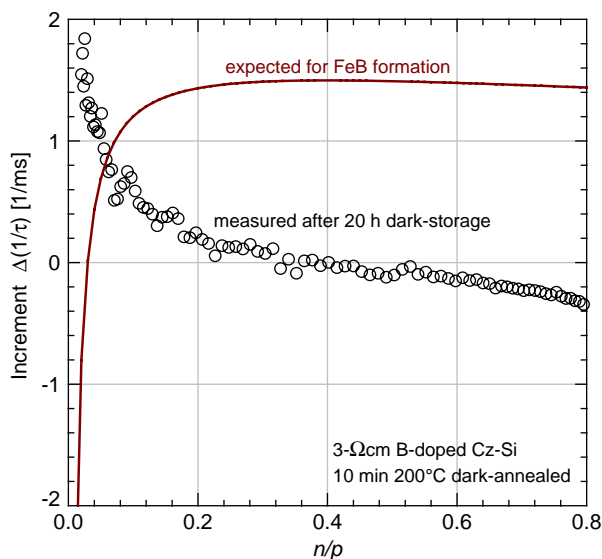


Figure 10. Increment in the reciprocal lifetime $\Delta(1/\tau)$ induced by a 20 h dark storage of the historic sample preannealed in the dark at 200 °C for 10 min (circles). The solid curve is a scaled calculated increment due to the pairing of Fe into FeB.

The recombination rate due to FeB is larger than that produced by isolated Fe if n is larger than about 10^{14} cm^{-3} —and smaller otherwise. Accordingly, the increment $\Delta(1/\tau)$ is positive at larger n/p and negative at smaller n/p values. The computed increment was scaled to be in the same order of magnitude as the measured increment shown by circles. Clearly, the dependence of the measured increment on n/p is opposite to that expected for the Fe to FeB conversion. This means that any possible effect of switching between Fe and FeB on the measured lifetime is screened by some other defect reaction.

Hence, we applied an additional methodology to estimate the iron content in our historic samples, as described in detail by Macdonald et al.,^[35] where the dissociated state of the FeB pairs is realized by illumination (in our case, performed at 0.5 suns for 5 min) and the associated FeB state is realized by room-temperature storage in the dark for >24 h. The measured lifetime change on the historic samples was <10%, and it was hence within the measurement uncertainty only possible to derive an upper limit for the iron concentration of $4 \times 10^{10} \text{ cm}^{-3}$ for the historic samples. Despite being quite small, the FeB dissociation might still have some impact on the extracted Q values. This effect should, however, be the same for all examined dark annealing times, which is not the case. In particular for the short annealing times (10 s and 1 min), where in fact, the largest contribution of FeB dissociation would be expected, a Q value of 11 was extracted even after the shortest illumination time of 50 s, indicating that the FeB dissociation has no impact on the extracted Q values.

We note furthermore that evidence that the historic FRC is indeed a true part of the B–O system and cannot be an independent Fe-related effect is given by both the aforementioned observation of long-time room-temperature recovery of the partially degraded historic samples and the boron and oxygen

compositional dependence found for the concentration of this defect.^[4,5] Another indication, in addition to the compositional dependences of concentration, that the historic FRC cannot be Fe related but is a part of the B–O system is that the rate constant of

degradation transformation follows a p^2 dependence which is another characteristic property of the B–O system.^[12]

Finally, another characteristic of the B–O system which distinguishes it from FeB pairing is that, as mentioned earlier, the B–O degradation rate constant is independent of the electron concentration n , with the exception of a very low n corresponding to light intensities less than 0.01 sun. On the contrary, it is well known that the dissociation rate of FeB pairs increases quadratically with increasing illumination intensity.^[36] Time-resolved lifetime degradation was examined by MW-PCD at two very different illumination (bias light) intensities, namely 0.06 and 0.24 suns. We would hence expect a factor of 16 between the two intensities were FeB dissociation to be a cause of lifetime degradation over time. The measurements, however, resulted in the same rates for the two very different intensities, again fully consistent with it being a part of the B–O system.

3. Advanced Degradation Model

The results for the aforementioned historic samples show that

- 1) RC_1 (SRC) is not the only emerging RC; there is at least one more emerging RC, with an essentially larger Q (seemingly close to 80). This one, labelled RC_2 (which is a reconfiguration of a corresponding LC_2), corresponds to what we previously labelled “FRC”.
- 2) Along with the production of two kinds of RCs (RC_1 and RC_2), there is also the disappearance of another center RC_3 that is present in the annealed state. This is evidenced not only by an illumination-induced increase in τ after prolonged dark annealing (Figure 9), but also by a super-linear dependence shown by curve 1 in Figure 8: a combination of only RC_1 and RC_2 would always result in a sublinear dependence, since the relative contribution of RC_2 (with a much larger Q) is quickly reduced at larger n/p .

Within this general notion, the increment in the reciprocal lifetime in Equation (1) is expressed as a combination of three terms:

$$1/\tau_{RC} = 1/\tau_1 + 1/\tau_2 - 1/\tau_3 \quad (5)$$

where $1/\tau_1$ is the contribution of the first center (RC_1 with $Q_1 = 11$), $1/\tau_2$ is that of the second center (RC_2 with $Q_2 = 80$, previously labelled as FRC), and $1/\tau_3$ is that of the disappearing center RC_3 (prior to their disappearance). Note that in our model described here, we assume that the silicon nitride surface passivation does not show any light-induced changes on the respective timescale, as verified on reference Fz-Si samples, and the Fe-related effects are not directly involved (see discussion in Section 2.4). Each lifetime on the right-hand side of Equation (5) is described by a linear dependence of Equation (2), with Q

equal to Q_1 , Q_2 , or Q_3 . The values Q_1 and Q_2 have been specified. A good fit to the $\tau_{RC}(n/p)$ curves in Figure 7 and 8 can be obtained adopting various values for the parameter Q_3 in some range provided Q_3 is well smaller than $Q_1 = 11$. We select a tentative value $Q_3 = 3$ that gives a somewhat better fit.

The solid curves in Figure 7 and 8 are computed using Equation (5) with the best-fit amplitudes A_1 , A_2 , and A_3 .

The time dependence of the deduced three amplitudes is shown in Figure 11. The amplitude A_1 of the RC_1 center again increases in two stages, a fast one and a slow one, and it is described by Equation (3) with the same timescales of $t_f = 1.25$ min and $t_s = 200$ min that have been deduced above. However, now the slow stage is dominant—contributing to 90% of the total saturated value of A_1 . Hence, most of the LC^* state has already been converted into LC after 5 min of dark annealing, and accordingly the conversion time $LC^* \rightarrow LC$ is between 1 and 5 min—according to our estimation ≈ 3 min (at 200 °C). The amplitude A_2 of RC_2 shows an initial increase, with a time constant of about 1 min (close to t_f), and this center is then dominant (i.e., has the largest amplitude). Subsequently, however, $A_2(t)$ decreases with a time constant of 90 min. The amplitude A_3 of the disappearing RC_3 is scattered around 0.7 ms^{-1} , not showing any definite trend. Therefore, the timescale for the RC_3 disappearance is well shorter than the smallest applied illumination time of 100 s. Although A_3 is much smaller than A_1 and A_2 , the LC_3 is essential for the injection-level dependence at high n/p values.

One important experimental finding is that in modern phosphorus-gettered Cz-Si samples, only one kind of RC is produced (namely RC_1)—both at the fast and slow stages of degradation. Still, there is a common feature of the modern and the historic samples: after a short dark preanneal, degradation occurs within a fast stage producing the same RC_1 .

We conclude that a simple degradation path, as shown in Figure 2 and 3, is common for historic and modern samples. In a modified notation, the RC in these figures should be labelled

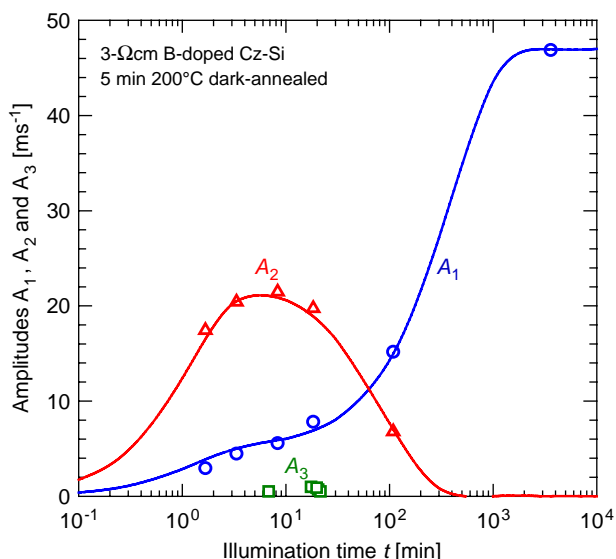


Figure 11. Evolution of the amplitudes A_1 , A_2 , and A_3 corresponding to the centers RC_1 , RC_2 , and RC_3 . The amplitudes were determined by fitting the curves of Figure 7 by Equation (5).

RC_1 . In the historic samples, however, there is another reaction path, taking place in parallel, involving the disappearance of RC_3 and the emergence of RC_2 . A proposed degradation/recovery scheme for this additional path—very similar to that of Figure 1—is shown in Figure 12. By a short dark anneal, RC_1 is converted into LC^* (Figure 1b or 2b). The RC_2 state is not converted directly into its latent precursor LC_2 since, after a short dark anneal, a subsequent degradation produces only RC_1 but not RC_2 . Hence, by a short dark anneal, the RC_2 reconfigures into the neutral state NC_3 (Figure 12b). A longer dark anneal leads to the conversion of NC_3 into RC_3 and then to an equilibration between RC_3 and LC_2 . The population of defects in Figure 12b will then include both RC_3 and LC_2 .

Therefore, a short dark anneal creates a strongly nonequilibrium population of defect states: mostly LC^* and NC_3 ; a subsequent degradation is a single-stage fast conversion of LC^* into RC_1 . A longer dark anneal creates an equilibrium population of LC , LC^* , LC_2 , and RC_3 . During illumination, the lifetime changes by all the paths are shown in Figure 2a (or Figure 3a) and Figure 12a. The resulting $\tau_{RC}(n/p)$ function may be super-linear (Figure 8, curve 1) or linear but with a time-dependent apparent parameter Q (Figure 7). In Figure 7, a gradual decrease in apparent Q is caused by an increasing fraction of RC_1 in a mixed population of RC_1 and RC_2 .

A possible reason for the absence of the path of Figure 12 in modern Cz-Si samples will be discussed in the following sections.

4. Nature of the Lifetime-Degrading B–O Defects

The effective saturated SRC concentration (defined as $1/\tau_{RC}$ at a fixed n/p ratio, in the end of the slow stage) was found^[5] to be proportional to the boron concentration $[B]$ and squared oxygen concentration $[O]^2$. The same is true for the saturated concentration of the FRC (at the end of the fast-stage degradation). This

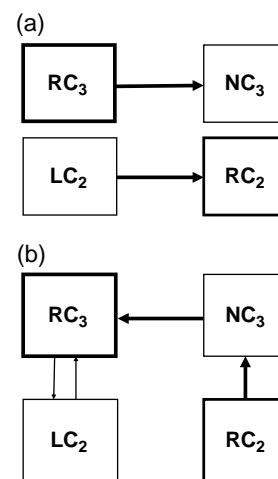


Figure 12. A transformation path presumably operating in the historic samples described in the study by Bothe and Schmidt^[4] for a) degradation and b) dark recovery. It involves RC_3 that is present in annealed samples—and disappears under illumination by conversion into a nonactive state NC_3 .

suggested a simple chemical composition of both lifetime-degrading centers^[5,37]: a BO_2 defect made up of a substitutional boron atom and an oxygen dimer. The once proposed involvement of interstitial boron^[22] now seems unlikely.^[37] Another possibility is that the defect includes BO_2 as a core and contains some unidentified impurity denoted as X ^[37]—implying that the defect is XBO_2 . The impurity X is assumed to be supplied by the impurity nanoprecipitates and thus have a definite concentration $[X]$ (the solubility) dependent only on T if X is neutral. BO_2 and XBO_2 species are formed^[37] during sample cooling from a high T , and their quenched-in concentration is proportional to $[B]$ and $[O]^2$. The concentration depends slightly on the cooling rate, being somewhat reduced by faster cooling. In the as-grown state, these defects are also present, being formed during crystal cooling. Within the XBO_2 model, the BO_2 defect itself does not give rise to lifetime degradation; for that, it should be first “activated” by attaching the X species.

If the “activating impurity” is positive (such as copper), the solubility $[X]$ is proportional to the hole concentration p_0 , and then the quenched-in concentration $[\text{XBO}_2]$ is proportional to $p_0 [B] [O]^2$ —or to $[B]^2 [O]^2$ in boron-only doped samples. Such a square dependence of SRC concentration on boron concentration was indeed found in one example^[38]—both before and after a very long-time dark equilibration at around 200 °C. Here, the hypothesis of the involvement of a positively charged activating impurity (such as copper) in the SRC defect would have been consistent with the experimental results. Our hypothesis is hence that there are different kinds of lifetime-degrading B–O defects, involving different activating impurities. The initially reported proportional dependence on boron^[4,5] corresponds to a neutral activator X , such as nickel, that has a very high diffusivity at low T .^[39]

For one particular kind of X activator—assumed to be present in the historic samples that were re-examined in this study—the degradation could proceed by the scheme of Figure 12, and this additional path creates the complicated behavior shown in Figure 7 and 8, and 9. In turn, this additional path may be related to a different level of purity. Modern Cz-Si materials have typically much lower metal contamination levels and the samples usually receive a phosphorus-gettering step, whereas the historic samples examined in the studies by Bothe and Schmidt^[4,5] were not gettered. Hence, they may contain additional, different activating impurities, most likely metallic ones.

5. Summary

There is an apparent dramatic conflict between the previous two-stage degradation data (with two kinds of RCs, FRC and SRC, produced in fast and slow stages, respectively) and more recent data (with a single SRC-like RC in both stages). By re-examining historic original B-doped Cz-Si samples, we have shown that, depending on the duration of a dark preanneal at 200 °C, and on the period of subsequent illumination, the FRC can be either a single one (previously labelled SRC) or a mixture of two centers. It should be emphasized here that while in this study we measured only one historical sample, it stands for an entire class of samples, many of which were measured over the course of many years. Along with the activation of the RCs (now labelled RC_1 and RC_2), there is clear experimental indication of a light-induced

disappearance of some other center (labelled RC_3) that is present in dark-annealed samples. The observed change in the lifetime as a function of the injection level is well reproduced by a model of three reactions (appearance of RC_1 and RC_2 and disappearance of RC_3), for various combinations of dark-annealing durations and illumination periods.

In modern Cz-Si samples, the degradation proceeds in a much simpler way—involving the activation of a single center RC_1 . The difference can be accounted for within a proposed concept of different kinds of activating impurities X attached to a BO_2 core defect. In this working hypothesis, each XBO_2 complex (for a particular activator X) can exist in several configurations, some recombination active and other nonactive. Under illumination (or in general electron injection) reconfiguration reactions occur, leading to either creation or disappearance of RCs. Each kind of X corresponds to its own reconfiguration pathway. One kind of “activator” X_a would be common for both historic and modern samples; it results in a two-stage activation of a single center RC_1 . Another kind of activator X_b would be specific for historic Cz-Si samples and give rise to RC_2 and RC_3 . The advanced defect model of LID proposed in this paper reconciles the historic and the modern data on the two-stage degradation. Future experiments designed to probe further the concepts developed here could be to selectively add Ni to the system following the phosphorus-gettering step by well-established means such as caustic etching^[40] and probe for the re-emergence of the large Q center. Similar experiments involving Cu could be performed using polishing.^[41]

Acknowledgements

J.S. and K.B. acknowledge the financial support by the German State of Lower Saxony.

Conflict of Interest

The authors declare no conflict of interest.

Keywords

defects, lifetime, light-induced degradation (LID), recombination, silicon

Received: March 20, 2019

Revised: July 26, 2019

Published online: August 25, 2019

- [1] H. Fischer, W. Pschunder, *Proc. 10th IEEE Photovoltaic Specialists Conf.*, IEEE, New York **1974**, p. 404.
- [2] J. Schmidt, A. G. Aberle, R. Hezel, *Proc. 26th IEEE Photovoltaic Specialists Conf.*, IEEE, New York **1997**, p. 13.
- [3] S. Rein, S. W. Glunz, *Appl. Phys. Lett.* **2003**, *82*, 1054.
- [4] K. Bothe, J. Schmidt, *J. Appl. Phys.* **2006**, *99*, 013701.
- [5] J. Schmidt, K. Bothe, *Phys. Rev. B* **2004**, *69*, 024107.
- [6] S. W. Glunz, S. Rein, W. Warta, J. Knobloch, W. Wettling, *Proc. 2nd World Conf. Photovolt. Solar Energy Conv.*, Joint Research Center European Commission, Ispra **1998**, p. 1343.
- [7] T. Saitoh, H. Hashigami, X. Wang, T. Abe, T. Igarashi, S. Glunz, S. Rein, W. Wettling, A. Ebong, B.M. Damiani, A. Rohatgi, I. Yamasaki,

- T. Nunoi, H. Sawai, H. Ohtuka, T. Warabisako, J. Zhao, M. Green, J. Schmidt, A. Cuevas, A. Metz, R. Hezel, *Proc. 16th European Photovolt. Solar Energy Conf.*, WIP, Munich **2000**, p. 1206.
- [8] K. Bothe, J. Schmidt, R. Hezel, *Proc. 29th IEEE Photovoltaic Specialists Conf.*, IEEE, New York **2002**, p. 194.
- [9] T. Schultz-Kuchly, J. Veirman, S. Dubois, D. R. Heslinga, *Appl. Phys. Lett.* **2010**, 96, 093505.
- [10] J. Geilker, W. Kwapil, S. Rein, *J. Appl. Phys.* **2011**, 109, 053718.
- [11] F. E. Rougieux, B. Lim, J. Schmidt, M. Forster, D. Macdonald, A. Cuevas, *J. Appl. Phys.* **2011**, 110, 063708.
- [12] V. V. Voronkov, R. Falster, K. Bothe, B. Lim, J. Schmidt, *J. Appl. Phys.* **2011**, 110, 063515.
- [13] J. Schön, T. Niewelt, J. Broisch, W. Warta, M. C. Schubert, *J. Appl. Phys.* **2015**, 118, 245702.
- [14] K. Ramspeck, S. Zimmermann, H. Nagel, Y. Gassenbauer, B. Birkmann, A. Seidl, *Proceedings 27th European Photovoltaic Solar Energy Conf.*, WIP, Munich, Frankfurt, Germany, **2012**, p. 861.
- [15] F. Fertig, K. Krauß, S. Rein, *Phys. Status Solidi RRL* **2014**, 9, 41.
- [16] D. Bredemeier, D. Walter, S. Herlufsen, J. Schmidt, *AIP Adv.* **2016**, 6, 035119.
- [17] K. Nakayashiki, J. Hofstetter, A. E. Morishige, T. Needleman, M. A. Jensen, T. Buonassisi, *IEEE J. Photovoltaics* **2016**, 6, 860.
- [18] H. Hashigami, M. Dhamrin, T. Saitoh, *Jpn. J. Appl. Phys.* **2003**, 42, 2564.
- [19] D. Macdonald, F. Rougieux, A. Cuevas, B. Lim, J. Schmidt, M. DiSabatino, L. J. Geerligs, *J. Appl. Phys.* **2009**, 105, 093704.
- [20] P. Hamer, N. Nampalli, Z. Hameiri, M. Kim, D. Chen, N. Gorman, B. Hallam, M. Abbott, S. Wenham, *Energy Proc.* **2016**, 92, 791.
- [21] A. Graf, A. Herguth, G. Hahn, *AIP Adv.* **2018**, 8, 085219.
- [22] V. V. Voronkov, R. Falster, *J. Appl. Phys.* **2010**, 107, 053509.
- [23] K. Bothe, J. Schmidt, *Appl. Phys. Lett.* **2005**, 87, 262108.
- [24] B. Lim, V. V. Voronkov, R. Falster, K. Bothe, J. Schmidt, *Appl. Phys. Lett.* **2011**, 98, 162104.
- [25] B. Hallam, M. Abbott, T. Narland, S. Wenham, *Phys. Status Solidi RRL* **2016**, 10, 520.
- [26] B. Hallam, M. Kim, M. Abbott, N. Nampalli, T. Narland, B. Stefani, S. Wenham, *Sol. Energy Mater. Sol. Cells* **2017**, 173, 25.
- [27] M. Kim, M. Abbott, N. Nampalli, S. Wenham, B. Stefani, B. Hallam, *J. Appl. Phys.* **2017**, 121, 053106.
- [28] M. Kim, D. Chen, M. Abbott, N. Nampalli, S. Wenham, B. Stefani, B. Hallam, *J. Appl. Phys.* **2018**, 123, 161586.
- [29] S. W. Glunz, S. Rein, W. Warta, J. Knobloch, W. Wettling, *Sol. Energy Mater. Sol. Cells* **2001**, 65, 219.
- [30] J. D. Murphy, K. Bothe, R. Krain, V. V. Voronkov, R. J. Falster, *ECS Trans.* **2013**, 50, 137.
- [31] T. Niewelt, S. Magdefessel, M. C. Schubert, *J. Appl. Phys.* **2016**, 120, 8.
- [32] T. Niewelt, J. Schön, W. Warta, S. W. Glunz, M. C. Schubert, *IEEE J. Photovoltaics* **2017**, 7, 383.
- [33] N. Nampalli, T. H. Fung, S. Wenham, B. Hallam, M. Abbott, *Front. Energy* **2017**, 11, 4.
- [34] L. C. Kimerling, J. L. Benton, *Physica* **1983**, 116B, 297.
- [35] D. H. Macdonald, L. J. Geerligs, A. Azzizi, *J. Appl. Phys.* **2004**, 95, 1021.
- [36] L. J. Geerligs, D. Macdonald, *Appl. Phys. Lett.* **2004**, 85, 5227.
- [37] V. V. Voronkov, R. Falster, *Phys. Status Solidi C* **2016**, 13, 712.
- [38] D. Walter, R. Falster, V. V. Voronkov, J. Schmidt, *Sol. Energy Mater. Sol. Cells* **2001**, 65, 219.
- [39] J. Lindroos, D. P. Fenning, D. J. Backlund, E. Veriage, A. Gorgulla, S. K. Estreicher, H. Savin, T. Buonassisi, *J. Appl. Phys.* **2013**, 112, 204906.
- [40] D. Singa, *ECS J. Solid State Sci. Technol.* **2018**, 7, N55.
- [41] S. Lee, S. Lee, Y. Kim, J. Kim, D. Hwang, B. Lee, *Bull. Korean Chem. Soc.* **2011**, 32, 2227.